Time-resolved spectroscopy of multiexcitonic decay in an InAs quantum dot

Charles Santori, Glenn S. Solomon,* Matthew Pelton, and Yoshihisa Yamamoto[†]

Quantum Entanglement Project, ICORP, JST, Edward L. Ginzton Laboratory, Stanford University, Stanford, California 94305
(Received 14 July 2001; revised manuscript received 12 October 2001; published 1 February 2002)

The multiexcitonic decay process in a single InAs quantum dot is studied through high-resolution time-resolved spectroscopy. A cascaded emission sequence involving three spectral lines is seen that is described well over a wide range of pump powers by a simple model. The measured biexcitonic decay rate is about 1.5 times the single-exciton decay rate. This ratio suggests the presence of selection rules, as well as a significant effect of the Coulomb interaction on the biexcitonic wave function.

Electrostatic interactions play an important role in the energy structures of semiconductor quantum dots[1] containing multiple particles. Although these interactions are usually treated as small perturbations to the single-particle wave functions, they lead to significant energy shifts that have been measured.[2–5] These effects offer possibilities for new quantum optical devices such as single-photon sources,[6,7] entangled photon sources,[8] and perhaps even a method to implement quantum logic.[9]

Single-exciton and multiexciton states, generated by adding electron-hole pairs to a dot, are of special interest for optical experiments. They are ideally the only states that can be generated through resonant optical excitation of quantum-dot transitions, and they also appear to be the states most commonly seen in above-band excitation experiments. Identification of individual multiexcitonic emission lines was originally based on the dependence of the emission intensity on the laser excitation power. More recently, time-resolved measurements on single quantum dots have become possible,[10–12] and measurements of biexcitonic emission from single CdSe dots[13] and multiexcitonic emission from ensembles of CdSe and CuCl nanocrystals[14,15] and single InAs dots[16] have been performed.

Here, we report high-resolution time-resolved measurements on a single InAs dot using a streak camera system. After identifying the single-exciton and multiexciton emission lines, we measure their decay rates, and find that the ratio of the one-exciton and biexciton decay rates is about 1:1.5. This is closer to the ratio expected for independent exciton recombination (1:2) than ratios reported for other material systems.[13–15] This result suggests the presence of strong selection rules, as well as a significant effect of the Coulomb interaction on the wave functions of multiexciton states. We finally show that the data may be well fitted over a wide range of excitation powers using a simple model.

The InAs self-assembled quantum dots used in this study were grown by molecular-beam epitaxy at a high temperature (520°C) to increase alloying between the InAs and the surrounding GaAs, yielding ground-state emission wavelengths in the range of 860–900 nm. The potential wells of the dots are thus rather shallow, and even the first excited states are close in energy to the wetting layer. The dots are approximately 30 nm wide, with a density of about 11 μm^{-2}. Small mesas (200 or 400 nm diameter) were then fabricated by electron-beam lithography and plasma etching

to isolate single dots. Mesas containing exactly one dot were identified through their optical-emission spectra. The spectra shown in Figs. 1(a), 1(b) were obtained from two mesas (mesas A and B, respectively) that have similar emission patterns, under continuous-wave (CW) excitation above the GaAs band gap (655-nm excitation wavelength). We identify the lines labeled 1 and 2 as one-exciton and two-exciton emission, since their dependences on excitation power are linear and quadratic, respectively, and since photon correlation measurements have confirmed their link. The lines labeled 1′ and 1″ have linear pump power dependence, but are identified as charged-state[17] emission, since they disappear under excitation resonant with a higher energy level in the dot, as is seen in Fig. 1(c).

Single mesas at a temperature of 5 K were excited from a steep angle (54° from normal) by 3 ps pulses every 13 ns from a Ti-sapphire laser, focused down to an 18-μm effective spot diameter. The resulting emission was collected by an NA (numerical aperture) = 0.5 aspheric lens, spectrally filtered to reject scattered laser light, and imaged onto a removable pinhole, which selected emission from a 5-μm region of the sample. The emission was then sent to an alignment camera, a spectrometer, or a streak-camera system,
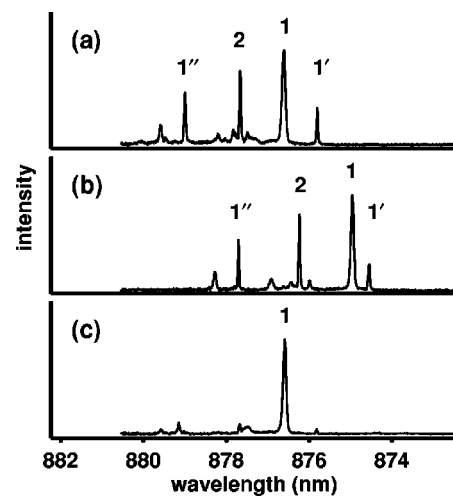

FIG. 1. Emission spectra of (a) mesa A and (b) mesa B under CW, above-band (655 nm) excitation, and (c) of mesa A under CW, resonant (858 nm) excitation. Lines 1 and 2 are one- and two-exciton emission, respectively, while lines 1′ and 1″ are believed to be charged-exciton emission.
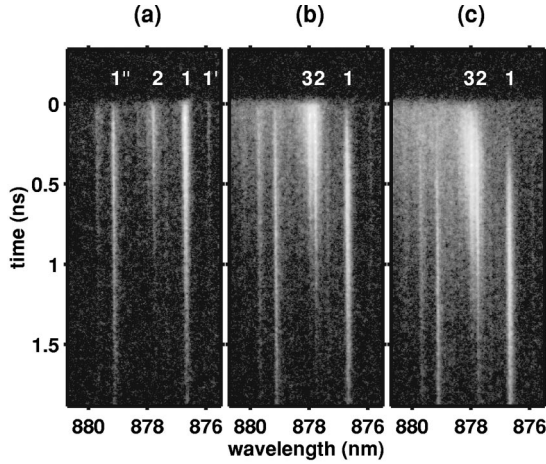
FIG. 2. Streak-camera images of emission from mesa A under pulsed, 708 nm laser excitation with powers (a) 27 μW, (b) 108 μW, and (c) 432 μW. For larger powers, a cascaded emission is seen, with the multiexcitonic emission (lines 2, 3) occurring first, followed by one-exciton emission (line 1).

which included a monochromator that determined both the spectral (0.13 nm) and temporal (25 ps) resolutions. The streak camera recorded the emission following the excitation pulses, averaged over about 5 min (2.3×10^{10} pulses). The resulting images were corrected for dark current, nonuniform sensitivity, and a small number of cosmic-ray events.

Images obtained under above-band (708 nm), pulsed laser excitation of mesa A with three different excitation powers are shown in Fig. 2. The observed emission lines are labeled as in Fig. 1. Figure 2(a) shows that under weak excitation (27 μW), the single-exciton line (line 1) appears less than 0.1 ns after the excitation pulse, and then decays exponentially. We attribute the small initial delay to the time required for electrons and holes generated by the excitation pulse to be captured by the dot. However, when the excitation power is increased to 108 μW, Fig. 2(b) shows that line 1 reaches its maximum only after a delay of about 0.5 ns. Most of the emission immediately after the excitation pulse now comes from the multiexciton lines 2 and 3. In this case, the laser pulse initially creates several electron-hole pairs, and some time is required before the population in the dot reduces to one electron-hole pair, after which one-exciton emission occurs. Under strong excitation (432 μW), one can see from Fig. 2(c) that the delay in the one-exciton emission is even longer, and a delay also appears for lines 2 and 3. Only the broadband emission in the vicinity of the multiexciton lines is seen to appear immediately after the excitation pulse.

The multiexcitonic decay process may be described by the following rate equation:

$$\frac{d}{dt} P_n(t) = \gamma_{n+1} P_{n+1}(t) - \gamma_n P_n(t), \qquad (1)$$

where $P_n(t)$ is the probability that n electron-hole pairs exist in the dot at time t, and γ_n is the decay rate of the n-pair state. The creation of charged-dot states is not considered here. Instead, we apply this model only to neutral-dot outcomes following an excitation pulse by excluding emission

lines 1′ and 1″ from the analysis, and noting that radiative decay beginning with a neutral state cannot generate charged states. The form of γ_n depends strongly on the nature of the states of the system. For an uncorrelated system with no recombination selection rules, one might expect $\gamma_n = n^2 \gamma_1$. For a dot much smaller than the exciton Bohr radius, the Coulomb interaction has little effect on the wave functions of multiexciton states, and due to selection rules one expects approximately independent recombination, $\gamma_n = n \gamma_1$. For a larger dot, it has been predicted that the Coulomb interaction produces a spatial separation between holes in multiexciton states, so that, for example, the biexciton state resembles a molecule.[13,18] In this case, one expects $\gamma_n < n \gamma_1$, and this has been observed for CdSe quantum dots.[13]

The decay rates γ_n in Eq. (1) can be measured directly from the time-dependent intensities of the lines corresponding to $P_n(t)$, when $P_n(t) \gg P_{n+1}(t)$. To perform this measurement as accurately as possible, we tuned the excitation laser to a resonance at about 858 nm, as in Fig. 1(c), creating electron-hole pairs directly inside the dot, which rapidly relax to a lowest energy state. This way, the delayed capture of electrons and holes, which can alter the apparent decay rates, does not occur, as it could in the above-band excitation case. The excitation power (about 2 mW) was chosen so that multiexciton states were created with significant probability. The intensities of lines 1, 2, and 3 were calculated in a straightforward manner, by integrating the streak camera image over strips about 0.2 nm wide, defined to include all of the emission from each line. Lines 2 and 3 were not completely resolved, and the integration boundary was placed midway between them. A further concern for the multiexciton lines 2 and 3 is that any weak background emission related to the one-exciton or charged-exciton states having a slower decay will cause significant distortion at large t, which is where we must measure the decay rates. With these cautions in mind, Fig. 3(a) shows the time-dependent intensities of lines 1, 2, and 3 under resonant excitation and a 60-min integration, plotted on a semilogarithmic scale. The slopes are estimated over the indicated regions by least-squares exponential fits. The time constants obtained are 0.479 ns, 0.316 ns, and 0.248 ns, respectively. The one-exciton (line 1) lifetime seen here is close to the value of 0.47 ns we have measured with weaker excitation powers. We obtain $\gamma_2 = 1.52 \gamma_1$, a result in between the small-dot limit ($\gamma_2 = 2 \gamma_1$) and what has been reported for CdSe dots ($\gamma_2 \approx \gamma_1$).[13] This is consistent with the presence of selection rules and a departure from the small-dot limit, due to the influence of the Coulomb interaction on the multiexciton wave functions. Line 3 is likely due to emission from the three-exciton state, since its wavelength relative to the one-exciton and biexciton lines is similar to what has been reported elsewhere for the three-exciton line,[19] and this identification is made plausible here by its time dependence. With this assumption, we obtain $\gamma_3 = 1.93 \gamma_1$.

We now wish to model the multiexcitonic decay process under above-band excitation over a wide range of excitation powers, to show that the behavior of lines 1, 2, and 3 is consistent with a cascaded decay. We assume that photons from the laser excitation pulse are absorbed independently
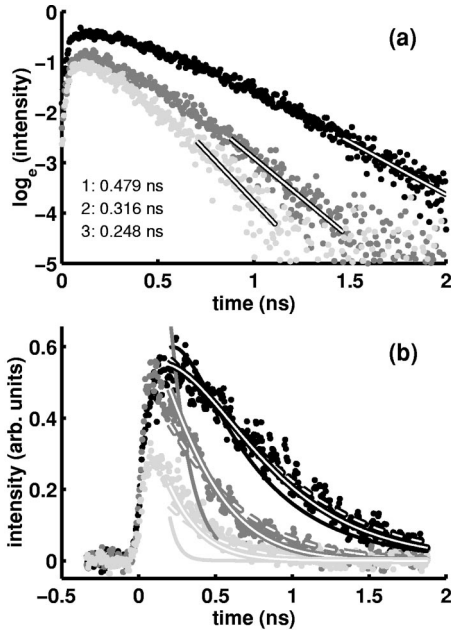
FIG. 3. (a) Time-dependent intensities of lines 1 (black), 2 (dark gray), and 3 (light gray) from mesa *A* under pulsed, resonant (858 nm, 2 mW) laser excitation. Exponential fits are applied after sufficient decay has occurred to estimate the decay times. (b) Time-dependent intensities under above-band (708 nm, 54 μW) excitation, compared to three models: $\gamma_n = n\gamma_1$ (hollow lines), measured decay rates (hollow, dashed), and $\gamma_n = n^2\gamma_1$ (solid).

FIG. 4. Time-dependent intensities of lines 1 (black), 2 (dark gray), and 3 (light gray) from mesa *A* under pulsed, 708-nm laser excitation with powers (a) 27 μW, (b) 54 μW, (c) 108 μW, and (d) 432 μW. Hollow lines show model fit results, and fit parameters are given at upper right.

by the GaAs surrounding the dot to form electron-hole pairs, and that these pairs are then independently captured by the dot, so that the initial population of the dot follows a Poisson distribution with mean μ. The dot then decays according to Eq. (1), and we assume that the observed intensity from the *n*-exciton state is $I_n = \gamma_n I_0 P_n$, where I_0 includes the collection efficiency. We make this assumption for simplicity, though it does not take into account the presence of multiple emission lines for $n > 2$. Figure 3(b) shows the time-dependent intensities of lines 1, 2, and 3 under above-band (708 nm, 54 mW) excitation, along with three models, each simultaneously fit to lines 1 and 2. The predicted three-exciton behavior is also shown, in comparison to line 3.

In the first model (hollow lines), we assume independent recombination, $\gamma_n = n\gamma_1$. Although this assumption differs substantially from the measured rates, its simplicity is appealing. The resulting time-dependent probabilities have the simple form of a Poisson distribution with exponentially decaying mean,

$$P_n(t) = (\mu e^{-\gamma_1 t})^n \exp(-\mu e^{-\gamma_1 t})/n!, \quad (2)$$

where μ is again the mean initial exciton number. This model is also well suited to handle an additional complication noticeable in the data. For above-band excitation, a finite time is required for the dot to capture the excitons generated by the laser pulse, with some recombination occurring during this time. But since, in this model, the excitons are both generated and annihilated independently, a Poisson distribution always holds, and it is sufficient to wait until the capture process has finished (0.2 ns) to begin fitting the data to Eq.
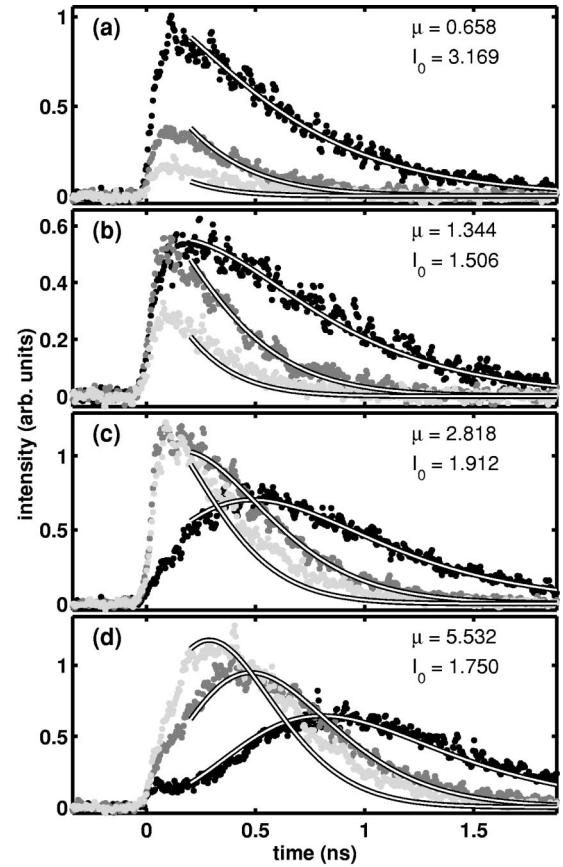
(2). In the second model (hollow, dashed lines), Eq. (1) is solved numerically, using the measured decay rates and assuming an initial Poisson distribution, beginning at 0.2 ns. The rates γ_n for $n > 3$ had to be extrapolated from the trend seen for $n \leq 3$, but have little effect on the result for this excitation power. In the third model (thin solid lines), Eq. (1) is solved numerically assuming $\gamma_n = n^2\gamma_1$, as one would expect with no recombination selection rules. For all the three models, only two fitting parameters are used, the initial mean number of excitons μ and the collection efficiency constant I_0. From these two fitting parameters, all three curves (one exciton, biexciton, three exciton) are obtained simultaneously. Two of these cascaded decay models, the model with independent exciton decay ($\gamma_n = n\gamma_1$) and the model using measured decay rates, fit the data reasonably well (mean-squared errors 8.2×10^{-4} and 9.4×10^{-4}, respectively). The other model ($\gamma_n = n^2\gamma_1$) fits the data poorly (mean-squared error 4.4×10^{-3}).

To demonstrate that lines 1, 2, and 3 are well described by a cascaded emission process, we fit the simplest model ($\gamma_n = n\gamma_1$) to the data for four different pump powers in Fig. 4. The value of γ_1 was fixed at $(0.47 \text{ ns})^{-1}$, and the obtained values of the fitting parameters I_0 and μ are shown. The value of μ increases linearly with excitation power at first,

and then begins to saturate. Ideally, I_0 should be the same for each streak-camera image, but in our case, we had to fit it separately for each image due largely to spatial sample drift and streak-camera gain drift. The fit was performed to minimize the combined errors for lines 1 and 2. For all the three lines, the simple model provides excellent agreement with the data in the weak, moderate, and strong-excitation cases, supporting the presence of a multiexcitonic decay sequence involving these lines.

In summary, we have observed multiexcitonic decay spectra from a single quantum dot using a streak camera, providing high temporal resolution. We have measured the decay rates of several lines, and found that the biexciton decay rate is about 1.5 times the one-exciton decay rate, suggesting strong recombination selection rules and a significant influence of the Coulomb interaction on the multiexciton wave functions. We then showed that, under above-band excitation, the time dependence of the emission lines is well described over a wide range of excitation powers by a simple model for cascaded emission.

---

*Also at Solid-State Photonics Laboratory, Stanford University, Stanford, CA.

†Also at NTT Basic Research Laboratories, Atsugishi, Kanagawa, Japan.

[1] D. Bimberg, M. Grundmann, and N. N. Ledentsov, *Quantum Dot Heterostructures* (Wiley, Chichester, 1999).

[2] A. Kuther, M. Bayer, A. Forchel, A. Gorbunov, V.B. Timofeev, F. Schäfer, and J.P. Reithmaier, Phys. Rev. B **58**, R7508 (1998).

[3] H. Kamada, H. Ando, J. Temmyo, and T. Tamamura, Phys. Rev. B **58**, 16 243 (1998).

[4] L. Landin, M.S. Miller, M.-E. Pistol, C.E. Pryor, and L. Samuelson, Science **280**, 262 (1998).

[5] M. Bayer, O. Stern, P. Hawrylak, S. Fafard, and A. Forchel, Nature (London) **405**, 923 (2000).

[6] C. Santori, M. Pelton, G. Solomon, Y. Dale, and Y. Yamamoto, Phys. Rev. Lett. **86**, 1502 (2001).

[7] P. Michler, A. Kiraz, C. Becher, W.V. Schoenfeld, P.M. Petroff, L. Zhang, E. Hu, and A. Imamoğlu, Science **290**, 2282 (2000).

[8] O. Benson, C. Santori, M. Pelton, and Y. Yamamoto, Phys. Rev. Lett. **84**, 2513 (2000).

[9] F. Troiani, U. Hohenester, and E. Molinari, Phys. Rev. B **62**, R2263 (2000).

[10] Ph. Roussignol, W. Heller, A. Filoramo, and U. Bockelmann, Physica E (Amsterdam) **2**, 588 (1998).

[11] V. Zwiller, M.-E. Pistol, D. Hessman, R. Cederström, W. Seifert, and L. Samuelson, Phys. Rev. B **59**, 5021 (1999).

[12] D.V. Regelman, E. Dekel, D. Gershoni, W.V. Schoenfeld, and P.M. Petroff, Phys. Status Solidi B **224**, 343 (2001).

[13] G. Bacher, R. Weigand, J. Seufert, V.D. Kulakovskii, N.A. Gippius, A. Forchel, K. Leonardi, and D. Hommel, Phys. Rev. Lett. **83**, 4417 (1999).

[14] V.I. Klimov, A.A. Mikhailovsky, D.W. McBranch, C.A. Leatherdale, and M.G. Bawendi, Science **287**, 1011 (2000).

[15] M. Ikezawa and Y. Masumoto, Phys. Rev. B **53**, 13 694 (1996).

[16] E. Dekel, D.V. Regelman, D. Gershoni, E. Ehrenfreund, W.V. Shoenfeld, and P.M. Petroff, Phys. Rev. B **62**, 11 038 (2000).

[17] J.J. Finley, P.W. Fry, A.D. Ashmore, A. Lemaître, A.I. Tartakovskii, R. Oulton, D.J. Mowbray, M.S. Skolnick, M. Hopkinson, P.D. Buckle, and P.A. Maksym, Phys. Rev. B **63**, 161305(R) (2001).

[18] T. Takagahara, Phys. Rev. B **39**, 10 206 (1989).

[19] A. Hartmann, Y. Ducommun, E. Kapon, U. Hohenester, and E. Molinari, Phys. Rev. Lett. **84**, 5648 (2000).